

Research Article

Research on Pattern Extraction Method of Underwater Acoustic Signal Based on Linear Array

Miao Yu , Yutong He, and Qian Kong

School of Electronic Information Engineering, University of Electronic Science and Technology of China, Zhongshan Institute, Zhongshan 528402, China

Correspondence should be addressed to Miao Yu; yumiao@zsc.edu.cn

Received 23 February 2022; Revised 22 March 2022; Accepted 23 March 2022; Published 15 April 2022

Academic Editor: Gengxin Sun

Copyright © 2022 Miao Yu et al. This is an open access article distributed under the Creative Commons Attribution License, which permits unrestricted use, distribution, and reproduction in any medium, provided the original work is properly cited.

Underwater acoustic signal is an important reference data for marine information research. The research and application of underwater acoustic signal have been widely concerned and valued by countries and enterprises. With the needs of modern military development and the development of marine industry, the research and application of underwater acoustic signal will develop faster and faster. In order to better understand marine information, it is necessary to collect seawater acoustic signal data. Aiming at the purpose of recording underwater acoustic signals placed in the ocean for a long time, this study innovates the calibration and recording of large dynamic range of long-time underwater acoustic signals, improves the circuit setting methods such as receiving, amplification, and sampling, designs a large dynamic series of long-time underwater acoustic signal recording device, and adopts the linear array extraction method, so that it can monitor the underwater acoustic biological sound under the condition of low power. It can also monitor the blasting sound of offshore engineering. Hardware circuit design mainly includes main control chip selection, amplification circuit design, filter circuit design, analog-to-digital conversion circuit design, storage circuit design, and some auxiliary circuit design. The fourth chapter introduces the software development process of large dynamic range underwater acoustic signal recorder and mainly introduces the system development tool, system clock working method, real-time clock module working method, underwater acoustic signal acquisition method, data storage scheme design, and the use of FatFs file system. The underwater acoustic signal data is stored on a MicroSD in the form of TXT file; linear array extraction method is used for feature extraction. Compared to other methods, the transformer will suppress DC and low-frequency interference signals, thus achieving high-pass filtering characteristics. Finally, the performance and experimental results of the whole underwater acoustic signal recording device are analyzed. After testing, the underwater acoustic signal recording device designed in this paper works stably and can record underwater acoustic signals with large dynamic range for a long time in low-power mode.

1. Introduction

The main nonanthropogenic hydroacoustic signals include marine vocalizations, earthquakes, volcanic eruptions, tides, ocean turbulence, waves, thunder, and other factors [1]. Currently, there are more than 25,000 species of fish in the marine environment, and when these fish communicate, hunt for food, swim, and do other activities, they will produce various kinds of hydroacoustic signals with different frequencies, most of which are concentrated between 30 Hz and 30 KHz; earthquakes, volcanic eruptions, tides, ocean turbulence, waves, thunder, and other geological

movements and weather factors will also lead to hydroacoustic signals in the ocean [2]. The frequency of these signals is relatively low and concentrated within 1 kHz. The hydroacoustic signals generated in the marine environment under man-made conditions are mainly underwater explosions, signals generated by surface ship navigation, hydroacoustic signals generated by marine development and military operations, and hydroacoustic signals generated by seaside industrial and construction activities [3]. Underwater blasting is one of the most important means of constructing coastal projects, and the acoustic signals generated by it vary in frequency from about 10 Hz to 105 Hz

during transmission due to the frictional and viscous forces of the water; ship navigation at the surface of the sea leads to the generation of hydroacoustic signals in the ocean from 5 Hz to 300 Hz; the development of the ocean and military activities, the sonar, torpedoes, and the signal covers all frequency ranges; various industrial and construction activities at the sea such as piling, dredging, ship construction, and harbor activities will have a certain effect on the hydroacoustic signal in the marine environment, which will be generated in the ocean in the frequency range of about 10 Hz to 10 KHz [4]. An important purpose of recording devices is to collect as many types of hydroacoustic signals as possible for analysis [5].

Another purpose of a large dynamic range hydroacoustic signal recording device is to capture a variety of hydroacoustic signals with varying signal strengths, except for signals generated by military activities, which are mostly generated in the ocean at frequencies of about 10 Hz to 30 kHz. In the process of sound generation by marine organisms, according to relevant data, the source level of signals from blue whales and fin whales (at 1 m from the source) can reach 190 dB; in the process of marine construction, the source level of signals generated by underwater explosions can reach 220 dB; in the process of marine exploration, the signals generated by various drilling equipment used are complex and the source level can reach 190 dB [6]. The source level of hydroacoustic signals generated in the ocean due to precipitation or high winds is 35 dB higher than the source level of the normal environment; the relative motion of ice on the sea surface can generate acoustic waves in large ice floes, while the mechanical stress of the rigid ice triggers the breakup of the ice to release strong acoustic waves; the source level of signals in the range of 10 Hz to 100 Hz was measured at a distance of 100 m from the active ice ridge and a water depth of 30 m [6]. The source level of the signal in the ocean varies greatly, and the location of the hydroacoustic signal recording device in the ocean also varies with the distance of the signal sources, resulting in different attenuation of the propagation process, and thus the intensity of the signals collected by the hydroacoustic signal acquisition device varies [7]. One of the objectives of this study is to solve this problem [8]. Considering the reason of the device, three channels are used in the design process of this study to collect the hydroacoustic signal, and the signal amplification rate is minimum 44 dB and maximum 160 dB [9].

The hydroacoustic signal recording device can be divided into four parts: large dynamic range conditioning module, digital processing module, system power module, and expansion interface module. The main function of the large dynamic range conditioning module is to process the hydroacoustic signals received by the hydrophone according to the technical requirements provided by the system, mainly including high-pass and low-pass filter circuits, gain amplification circuits, and AD conversion circuits; digital processing module mainly consists of STM32 main control chip and its peripheral circuits and MicroSD, through the programming of the hydroacoustic signals stored in the storage media; power module includes digital power supply

and analog power supply, for the entire device of various parts of the power supply; expansion interface module can provide other ways of debugging methods for the device and allows the device to communicate with other devices or similar products. The main function of the large dynamic range module is to clearly screen out the desired hydroacoustic signal. The filter circuit is designed to filter out the signal in the desired band and filter out the unwanted signal. The function of the gain circuit is to amplify the weak hydroacoustic signals collected by the hydrophone for reception. Since the strength of hydroacoustic signals in the ocean varies, multistage amplification is used for all hydroacoustic signals in the large dynamic range circuit in order to collect as much ocean information as possible and avoid loss of weak signals. The main content of this thesis is to study a large dynamic range hydroacoustic signal recording device, the main purpose of which is to record as many hydroacoustic signals as possible present in the marine environment in real time. The large dynamic range refers to the type of signal source collected on the one hand; on the other hand, it refers to the intensity of the collected signal.

The digital processing module is mainly composed of STM32 main control chip, its peripheral circuit, and MicroSD. It programs the underwater acoustic signal stored in the storage medium. The power module includes digital power supply and analog power supply to supply power to all parts of the whole equipment. The extended interface module can provide other debugging methods for the equipment and can also make the equipment communicate with other pieces of equipment or similar products.

2. Related Works

A dedicated circuit is designed between the input port and the output port according to the signal frequency range required by the output port. Using this circuit, the desired signal frequency is output from the output port, while the rest of the frequency is attenuated. This hardware circuit with frequency selection characteristics is called a filter in engineering. The passband in a filter is the range of frequencies that pass through the output port, and the stopband is the range of frequencies that are suppressed from the output port [10]. Filters are classified into four types based on their passband and stopband characteristics, specifically: four ideal filters with low-pass (LPF), high-pass (HPF), band-pass (BPF), and band-rejection (BEF) waveforms [11]. Filters are classified into active and passive filters based on whether they require power supply [12]. Passive filters are LC resonant circuits that use passive device resistors and capacitors to provide a low-impedance path for signals at a specific frequency [13]. This low-impedance path is connected in parallel and shunted with the system impedance, allowing harmonic components to be filtered out of the filter system [14]. Active filters filter the harmonics generated by the system by combining the characteristics of modern power electronics to autonomously generate a harmonic so that it is equal in size and opposite in phase to the system harmonics. Because of the presence of resistors,

inductors, and capacitors, the power consumption of passive filters is higher than that of active filters in the same situation, and the delay of the circuit is larger [15]. Active filters consume relatively little power and do not attenuate in the passband, while the amplification can be changed by setting the Q value of the filter.

For high signal processing, an active filter circuit is more appropriate than a passive filter circuit because the active filter circuit will not affect the filter characteristics due to load variations [16]. The passive filter circuit will affect its passband amplification factor and cutoff frequency due to load changes. Active filtering is effective and expensive; passive filtering is ineffective and cheap. The active filter circuit uses power electronics to detect the harmonic components of the system [17]. A set of harmonic components will be generated at the same time as the harmonics are detected, which are equal in amplitude and opposite in phase to filter the harmonic components of the system, and the filtering effect can reach 95%. Passive filter circuits provide a low-impedance path for harmonic currents by matching inductors and capacitors to filter out the desired harmonic components, with a filtering effect of about 80% [18]. Passive filters can cause harmonic amplification and resonance problems due to system impedance; active filters are not affected by this. A passive filter will cause the resonance point to shift due to frequency changes, but an active filter will not. Passive filters can be damaged by overload and vary with load; active filters are not at risk and are not affected by load variations.

The hydroacoustic signal received by the hydrophone first enters the high-pass filter circuit, which filters out low-frequency signals below 10 Hz. Since the high-pass filter has a cutoff frequency of 10 Hz and very low frequencies, it is not easy to use an active filter circuit but a passive filter. If the passive high-pass filter is converted according to the conversion mode of the normalized low-pass filter, the calculated values of the capacitor and inductor components will be large. It is not easy to find components in the market and the devices are large and not easy to design. This study directly uses an audio transformer to filter out the low-frequency signal. Audio transformers, also known as low-frequency transformers, operate in the frequency range of 10 Hz to 30 KHz, with the original winding inductance of the transformer determining the lowest frequency of the passband and the leakage inductance determining the highest frequency of the passband. Usually, a sufficient passband is ensured by increasing the original winding inductance and reducing the leakage inductance. During the operation of an audio transformer, a signal source containing a DC or low-frequency AC signal is fed to the primary side of the transformer. According to the transformer's operating principle, the transformer will suppress DC and low-frequency interference signals, thus achieving high-pass filtering characteristics. This design uses an ED8 chip audio transformer made of PoMo alloy nickel steel with an inductance of 1.2 H and a DC impedance ratio of 600:600 and an AC impedance ratio of 110:130.

3. Hydroacoustic Signal Pattern Extraction and Simulation

3.1. Hydroacoustic Signal Transmission. The main purpose of the hydroacoustic signal recording device designed in this study is to collect and store the hydroacoustic signal in the ocean, without transmitting the hydroacoustic signal to the outside, so the main theory used in this study is the passive sonar theory, and the workflow diagram of the passive sonar is shown in Figure 1. Expansion interface module can provide other ways of debugging methods for the device and allows the device to communicate with other devices or similar products.

In the applied research of passive sonar, the main theoretical study used is the following passive sonar equation:

$$SL - TL = DT - DI + NL, \quad (1)$$

where SL is the source level of the hydroacoustic signal, TL is the signal loss of the hydroacoustic signal in the propagation process, NL is the source level of the interference signal in the marine environment, DI is the signal reception directionality index in the signal reception process, and DT is the reception threshold of the hydroacoustic receiving equipment.

The specific definition of SL source level is the ratio between the signal intensity IN and the reference sound intensity I_0 measured by the hydrophone in the direction of the sound axis of the received hydroacoustic signal and at the location of the center of the target source; that is,

$$SL = 10 \log \left(\frac{I_N}{I_0} * 100\% \right). \quad (2)$$

TL signal propagation loss is specifically defined as the amount of change in the signal strength of an acoustic wave after propagation over a distance; that is,

$$TL = 10 \log \left(\frac{I_1}{I_r} * 100\% \right), \quad (3)$$

where I_1 refers to the signal intensity of the acoustic wave at 1 m from the center of the source and I_r refers to the signal intensity of the acoustic wave at a distance r from the source.

NL indicates the strength of the interference signal present in the marine environment and is specifically defined by the following formula:

$$NL = 10 \log \left(\frac{I_N}{I_0} * 100\% \right), \quad (4)$$

where I_N refers to the strength of the measured interference signal and I_0 refers to the signal strength of the reference acoustic wave. The specific definition of NL is given by

$$NL = 10 \log \left(\frac{I_N}{I_0} * 100\% \right). \quad (5)$$

In the relevant calculations, assuming that the source level of the signal is 230 dB (such as the explosion; this signal can be transmitted in all directions, so $DI = 0$), the standard

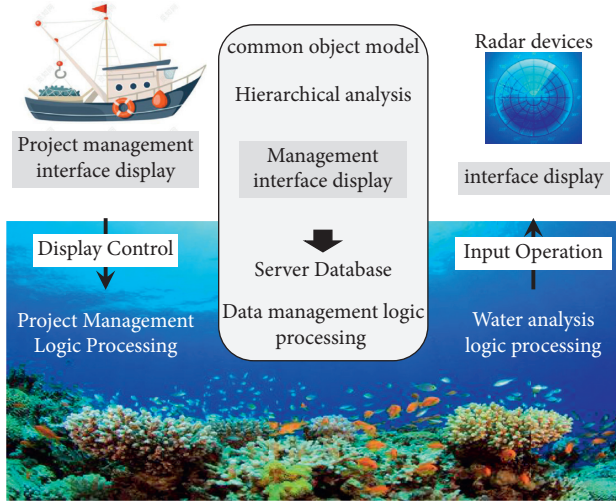


FIGURE 1: Flow chart of hydroacoustic information.

hydrophone TC4040 is selected for reception, and its sensitivity is 56 $\mu\text{V}/\text{Pa}$, with the maximum signal amplification of 160 dB.

1, calculate how far away the device can detect the signal.

The noise signal present in the marine environment is not considered, and only the propagation loss is considered during the propagation of the signal.

From what is known, we have

$$SL = 10 \log \left(\frac{Q_1}{Q_0} * 100\% = 230 \text{ dB} \right). \quad (6)$$

The analog-to-digital conversion module can receive a maximum signal of 5 V, which corresponds to a signal voltage of

$$P = \frac{5 \text{ V}}{102 \mu\text{V}/\text{Pa}} = 5000 \text{ Pa}. \quad (7)$$

Translating this into sound pressure levels yields

$$SLP = \log \left(\frac{5 \text{ V}}{102 \mu\text{V}/\text{Pa}} \right). \quad (8)$$

The losses resulting from the propagation of sound waves in seawater are mainly composed of expansion loss, absorption loss, and scattering loss. Compared with the other two losses, the scattering loss is negligible.

Therefore, the calculation formula of propagation loss is

$$TL = TL1 + TL2(\text{Loss}). \quad (9)$$

The expansion loss is calculated according to the equation for spherical waves; that is,

$$TL1 = 20gr * \log \left(\frac{r}{r_0} \right). \quad (10)$$

The absorption loss is calculated as

$$TL2(\text{Loss}) = 20\alpha * \log \left(\frac{r}{r_0} \right). \quad (11)$$

The hydroacoustic signal recording device can be divided into four parts: large dynamic range conditioning module,

digital processing module, system power module, and expansion interface module. The main function of the large dynamic range conditioning module is to process the hydroacoustic signals received by the hydrophone according to the technical requirements provided by the system, mainly including high-pass and low-pass filter circuits, gain amplification circuits, and AD conversion circuits; digital processing module mainly consists of STM32 main control chip and its peripheral circuits and MicroSD, through the programming of the hydroacoustic signals stored in the storage medium; power module includes digital power supply and analog power supply, for the entire device of various parts of the power supply.

3.2. Dynamic Conditioning and Linear Array Sequencing of Hydroacoustic Signals.

The main function of the large dynamic range module is to clearly mask out the desired hydroacoustic signal. The filter circuit is designed to filter out signals in the desired frequency band and filter out unwanted signals. The function of the gain circuit is to amplify the weak hydroacoustic signals collected by the hydrophone for reception. Since the strength of hydroacoustic signals in the ocean varies, multistage amplification is used for all hydroacoustic signals in the large dynamic range circuit in order to collect as much ocean information as possible and avoid loss of weak signals. The functional block diagram of the large dynamic range module design is shown in Figure 2. The low-frequency signal is filtered and passed through the amplification, low-pass filter circuit, and finally the digital signal with discontinuous time and amplitude is sent to the data processing module through the ADC circuit.

A dedicated circuit is designed between the input port and the output port according to the signal frequency range required by the output port. Using this circuit, the desired signal frequency is output from the output port, while the rest of the frequency is attenuated. This hardware circuit with frequency selection characteristics is called a filter in engineering. The passband in a filter is the range of frequencies that pass through the output port, and the stopband is the range of frequencies that are suppressed from the output port. Filters are classified into four types based on their passband and stopband characteristics, specifically: four ideal filters with low-pass (LPF), high-pass (HPF), band-pass (BPF), and band-rejection (BEF) waveforms as shown in Figure 3.

Then the minimum sound pressure level of the signal that can be received by the hydrophone is

$$\frac{219 - 160}{12} = 5 \text{ dB}. \quad (12)$$

According to the sonar equation, the propagation loss generated by the sound waves during the propagation is

$$\frac{280 - 160}{12} = 10 \text{ dB}. \quad (13)$$

Active filtering effect is good, and the cost is high; passive filtering effect is poor, and the cost is low. The active filter

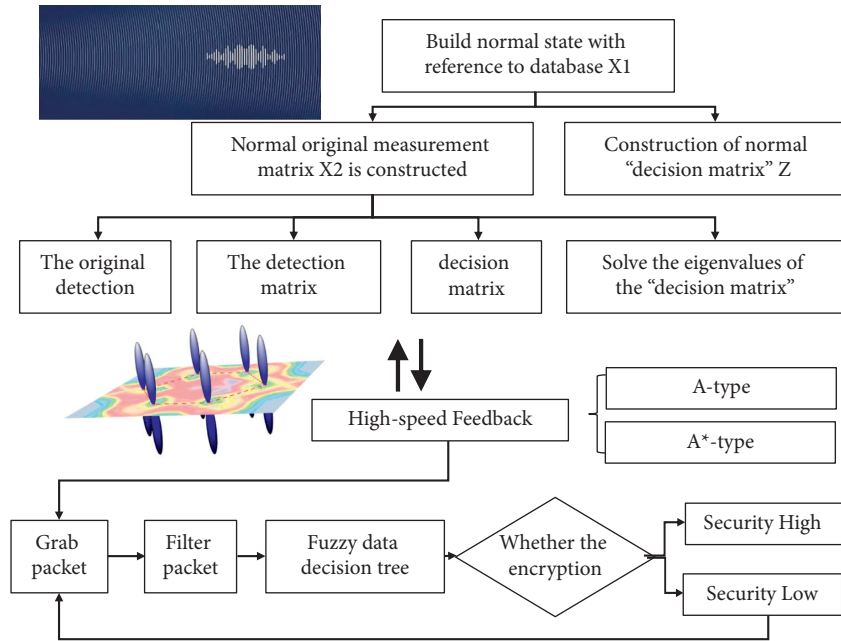


FIGURE 2: Functional block diagram of large dynamic range module.

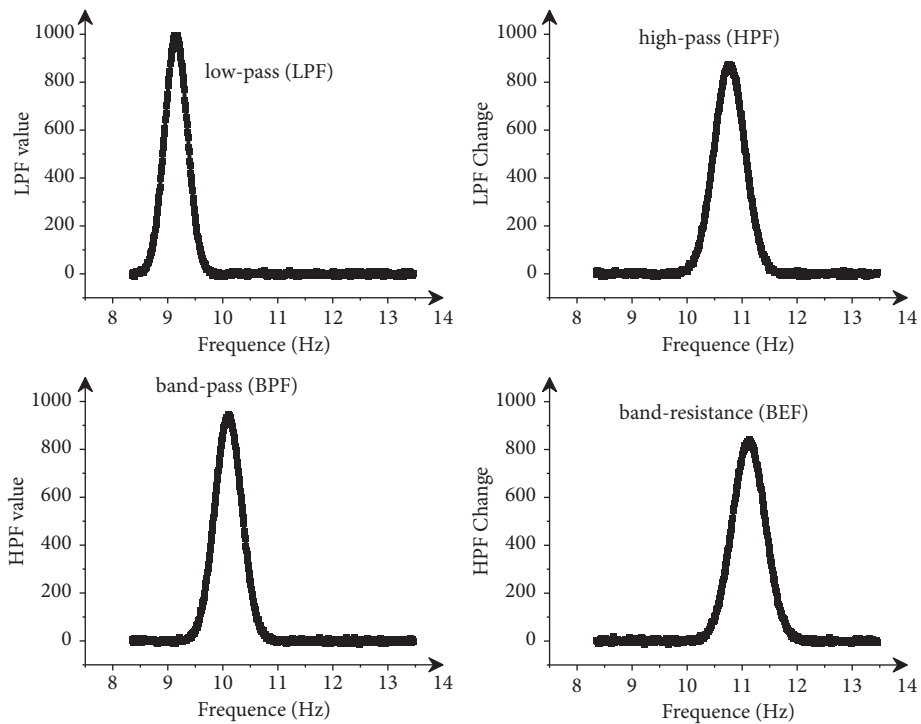


FIGURE 3: Array sorting results of hydroacoustic signals.

circuit uses power electronics to detect the harmonic components of the system.

Filters are classified as active and passive filters depending on whether or not they require power. Passive filters are LC resonant circuits that use passive device resistors and capacitors to provide a low-impedance path for signals of a specific frequency. This low-impedance path is

connected in parallel and shunted with the system impedance, allowing harmonic components to be filtered out of the filter system. Active filters filter the harmonics generated by the system by combining the characteristics of modern power electronics to autonomously generate a harmonic so that it is equal in size and opposite in phase to the system harmonics.

3.2.1. *The Filtering Principle Is Different.* The differences can be seen from above.

3.2.2. *Power Consumption Is Different.* Because of the presence of resistors, inductors, and capacitors, the power consumption is higher in the same case for passive filters than for active filters, and the delay of the circuit is larger. Active filters consume relatively little power and do not attenuate in the passband, while the amplification can be changed by setting the Q value of the filter.

3.2.3. *The Scope of Application Is Different.* For high signal processing, an active filter circuit is more appropriate than a passive filter circuit because the active filter circuit will not affect the filter characteristics due to load variations. The passive filter circuit will affect its passband amplification factor and cutoff frequency due to load variation.

3.2.4. *The Filtering Effect and Price Are Different.* A set of harmonic components are generated at the same time as the harmonics are detected, which are equal in amplitude and opposite in phase to filter the harmonic components of the system, and the effect of filtering can reach 95%.

3.2.5. *Impedance Influence.* Passive filters can cause harmonic amplification and resonance problems due to system impedance; active filters are not affected by this.

3.2.6. *Frequency Effect.* A passive filter will cause the resonance point to shift due to the change in frequency, but an active filter will not.

3.2.7. *Load Impact.* Passive filters can be damaged by overload and vary with the load; active filters are not at risk and are not affected by load variations.

3.3. *Filter Flux Design of Hydroacoustic Signal.* The water sound signal above 30 KHz is filtered out by low-pass filtering. Considering the power consumption, filtering effect, frequency, impedance, and other conditions, active filtering is selected for filtering, as shown in Table 1. In the design of the circuit, there is a way to effectively remove the interference signal, that is, decoupling capacitors added to the circuit power supply input and output terminals. All chips are connected between power and ground with good frequency characteristics of 10 μ F tantalum capacitors and in parallel with good high-frequency characteristics of 0.1 μ F nonpolarized small capacitors, as well as power supply bypass as close as possible to the power supply pins.

Main technical specifications of the low-pass filter are shown in Figure 4. Active filters filter the harmonics generated by the system by combining the characteristics of modern power electronics to autonomously generate a harmonic so that it is equal in size and opposite in phase to the system harmonics.

(12) The passband gain A_{vp} is the voltage amplification factor of the filtered signal in the passband. The performance of LPF is judged by the amplitude-frequency characteristic curve in the passband and the voltage amplification factor in the stopband.

As regards passband cutoff frequency, for LPF, f_p is its upper cutoff frequency. The transition zone is the boundary between the passband and the resistive band, and the narrower the transition zone, the better the filtering effect.

To make the high-frequency signal decay faster in the transition phase, an RC filter circuit can be added to the front end to meet the design requirements for system performance. For an ideal filter, it is practically difficult to implement and can only be approximated by the actual characteristics. According to the above approach, higher orders are required to obtain better filtering characteristics, but the computational problems associated with filter design are more troublesome.

3.4. *Signal Extraction Accuracy and Interference Test.* The main purpose of the signal amplification test is to ensure that the amplification factor of the amplifier circuit meets the design requirements for the hydroacoustic signal to pass through. The amplitude of the output signal after the signal receiving circuit meets the requirements of the analog-to-digital conversion acquisition circuit. The test was performed by using an oscilloscope to generate a sinusoidal signal with an amplitude of 10 mV and outputting it to the signal input of the signal receiving board. After high-pass filtering and the first-stage amplification circuit, the oscilloscope detects the waveform of the output signal and measures the amplitude of the output signal. The measured voltage output value is compared with the input signal. Two main points are tested in the test: the high-pass filter output and the first-stage amplifier output. Since the high-pass filter circuit is passively filtered, it also attenuates the signal. The data tested is shown in Figure 5. The passive filter circuit provides a low-impedance path for harmonic currents by matching inductors and capacitors to filter out the desired harmonic components, with a filtering effect of about 80% (note: the voltage measured in the table is the peak-to-peak value, and the input signal voltage is 20 mV peak-to-peak; Magnification 1: refers to the ratio of the signal to the input signal after passing through the high-pass filter circuit; Magnification 2: refers to the ratio of the output signal to the input signal after high-pass filtering and first-stage amplification; Magnification 3: refers to the ratio of the output signal to the input signal after amplification; total amplification: refers to the ratio of the output signal to the input signal after the first-stage amplification is estimated (the ratio of the output signal to the input signal after the second-stage and third-stage amplification of the output signal after the first-stage amplification)).

The main purpose of this test is to determine the integrity of a very weak seawater acoustic signal before it is input to the analog-to-digital converter circuit, after it has been filtered and amplified by the hydrophone and transmitted to the signal receiving board. In this paper, several sets of

TABLE 1: Amplitude modulation characteristics result statistics.

Amplitude modulation factor	Real-time communication	Control transfer
1	NA	0.39 ± 0.15
2	NA	0.72 ± 0.14
3	0.6213 ± 0.29	0.62 ± 0.19
4	0.6349 ± 0.23	0.6539 ± 0.15
5	0.7365 ± 0.13	0.8186 ± 0.29

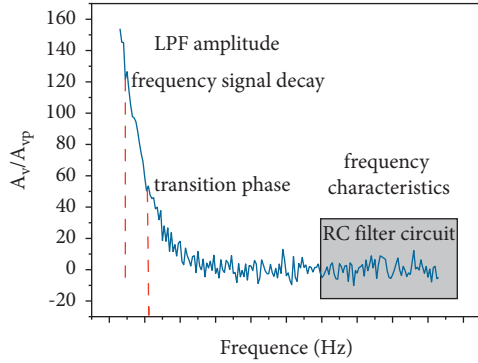


FIGURE 4: LPF amplitude and frequency characteristics curve.

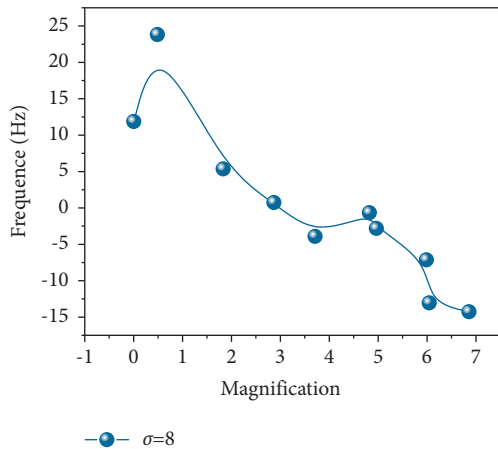


FIGURE 5: Magnification versus frequency curve.

sinusoidal signals of different frequencies with 10 mV amplitude in the frequency range are output from the signal generator to the signal receiving board. After filtering and amplification, the signals at the output of the primary amplifier circuit are detected using an oscilloscope. The interference signal generated in the system has an important impact on the stability of the work of the whole system device. In order to improve the stability of the work of the hydroacoustic signal recording device, the circuit needs to be reasonably designed to minimize or eliminate the possible existence of interference signals. The digital ground of the circuit is separated from the analog ground and connected by an inductor to reduce interference signals from the digital side into the analog terminals. In PCB wiring, power and ground lines are as thick as possible, which reduces voltage drop and, more importantly, coupled interference signals. Connect the ground signal on the board to the signal

receiving end and detect the signal waveform at the output after filtering and one stage of amplification circuit as Figure 6 shows.

As can be seen from the figure, the input signal is a random waveform with a peak-to-peak voltage of about 41.1 mV. The output signal is a rectangular waveform with a period of about 11.344 ms (88.15 Hz) and a peak-to-peak voltage of about 893.99 mV. This result explains why the signal amplification circuit amplifies rather than attenuates the output signal when the input signal is between 50 Hz and 150 Hz. Figure 7 shows the waveform displayed on the oscilloscope detection port connected to the ground side of the power supply. The figure shows that the signal is an irregular waveform with a peak-to-peak voltage of about 42.4 mV, which is similar to the grounded signal waveform.

In order to test the performance of the hydroacoustic signal data acquisition system designed in this project, our group placed the data acquisition system in the whole water depth monitoring system of a harbor channel for testing. Using the whole system in the Dalian sea, a large number of experiments were conducted in the harbor pond, two customized brackets were placed, the transmitting and receiving transducers were fixed on one bracket each with the same height and placed according to a certain inclination angle, the angle was determined according to the height and spacing of the transducers, the ultrasonic signal from the transmitting transducer was collected and processed by the system designed in this project after the reflection from the water bottom, and the mixed signal at the receiving end was judged to be the starting point n , and then the effective data of the water depth signal and the starting point position of the mixed signal will be sent to the upper computer together. The measurement time parameters of the whole system include the time from the time the transmitter unit detects the rising edge of the GPS (Global Positioning System) second pulse to the time of generating the ultrasonic signal with frequency of 200 K, the time from the time the receiver unit detects the rising edge of the GPS second pulse to the time of starting the high-precision timer, the time of the FPGA- (Field Programmable Gate Array-) based high-precision timer, the time from the time the microcontroller detects the end of timing to the time of starting the AD (analog digital) converter, and the time calculated according to the sampling of the high-speed acquisition system. The result is shown in Figure 8. According to the system test, the timing error of the high-precision timing module is less than 25 ns: the timing error of the GPS timing module is 25 ns; the response of the microcontroller to the second pulse and the AD start signal are interrupted, and the time measurement error of the whole system is less than 1 ns.

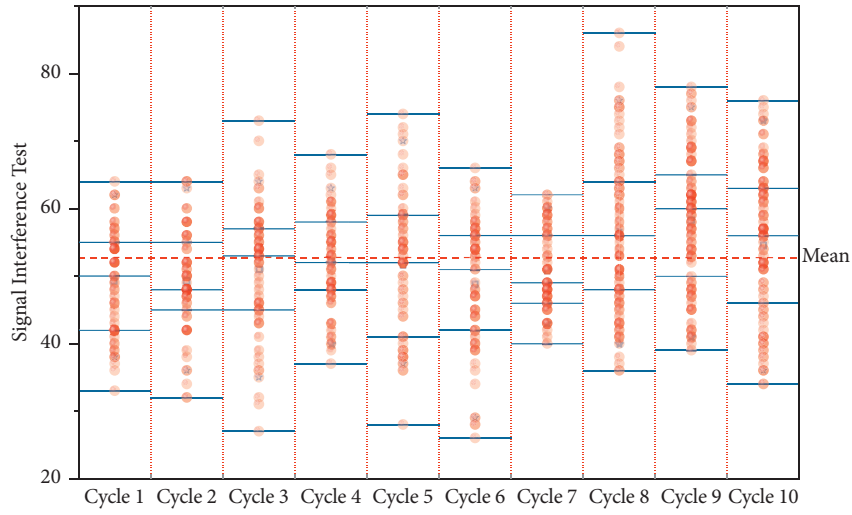


FIGURE 6: Signal interference test.

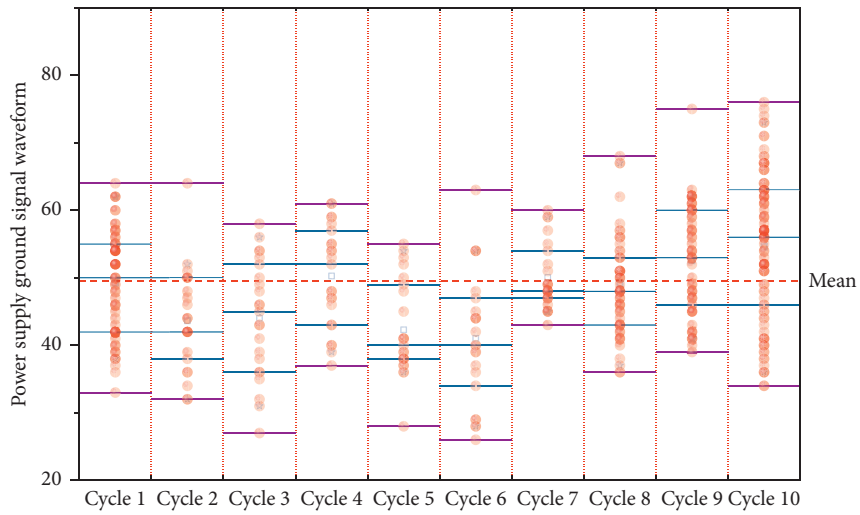


FIGURE 7: Detection of power supply ground signal waveform.

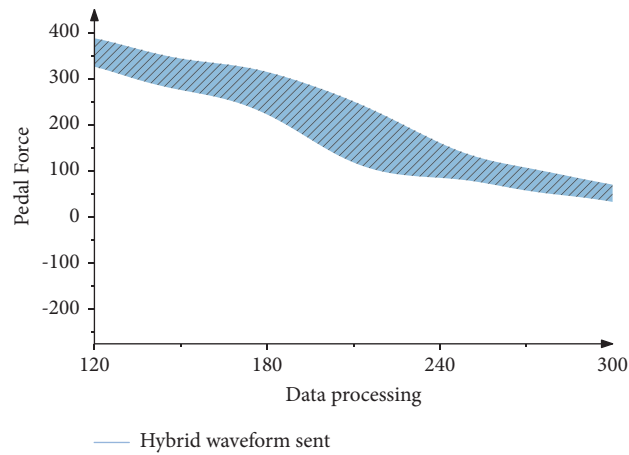


FIGURE 8: Hybrid waveform sent after data processing.

When using the short-time energy analysis method for data analysis, there is a contradiction in the choice of window width: when the sampling rate is certain, the shorter the window width, the higher the time resolution and the more accurate the judgment of the starting point of the hydroacoustic signal, but it is not conducive to play the characteristics of the short-time energy analysis of high signal-to-noise ratio. The error of high-precision timer is mainly caused by the stability of the crystal oscillator, the system uses a constant temperature crystal oscillator rather than the general ordinary crystal oscillator which can somewhat reduce the error caused by the stability of the crystal frequency, but this error is still inevitable. The short-time energy analysis method described in this paper is able to separate the starting point of the reflected waves of hydroacoustic signals by choosing the window width and the energy judgment gap value, but there is still a certain error in the determination of the starting point of the reflected waves of hydroacoustic signals. Because of the existence of resistance, inductance, and capacitance, the power consumption of the passive filter is higher than that of the active filter in the same situation, and the delay of the circuit is larger. Active filters consume relatively little power and do not attenuate in the passband, while the amplification can be changed by setting the Q value of the filter. For high signal processing, the active filter circuit is more suitable than the passive filter circuit because the active filter circuit does not affect the filter characteristics due to load variations. The passive filter circuit will affect its passband amplification factor and cutoff frequency due to load variation.

4. Conclusion

In this paper, a large dynamic range hydroacoustic signal recording device is developed, including the design of the system hardware circuit and the software programming that allows the device to work properly. This paper describes in detail the principle of operation and the functions of each hardware circuit module in the whole device, including filtering circuit, amplifier circuit, analog-to-digital conversion circuit, ARM chip hardware circuit, data acquisition circuit, and data storage circuit. The software design mainly includes ARM processing chip function implementation, system clock function setting, RTC real-time clock function implementation, and data storage program design. The whole system device contains two circuit boards: the signal receiving circuit board and the data processing and storage circuit board. The signal receiving circuit board is mainly responsible for filtering and amplifying the hydroacoustic signal to select the desired hydroacoustic signal. The external hydrophone acquires the hydroacoustic signal in the ocean through the hydrophone and transmits the appropriate signal to the analog-to-digital conversion circuit for conversion into a digital signal through the filtering and amplification circuit. The data processing storage board mainly handles the digital signals stored in the receiver circuit board. This design uses a FAT file management system to store the data in a TXT file on a MicroSD card.

In the future, the short-time energy analysis method described in this paper is able to separate the starting point of the reflected waves of hydroacoustic signals by choosing the window width and the energy judgment gap value.

Data Availability

The data used to support the findings of this study are available from the corresponding author upon request.

Conflicts of Interest

The authors declare that they have no known competing financial conflicts of interest or personal relationships that could have appeared to influence the work reported in this paper.

Acknowledgments

This work was supported by Youth Innovative Talents Program of Colleges and Universities of Guangdong Province (2018KQNCX332), Leading Talents Program of Guangdong Province Program (no. 00201507), Founding Project of Education Department of Guangdong Province (no. 2018KCXTD033), the Social Welfare Science and Technology Research Project of Zhongshan City (nos. 2018B1021 and 2020B2018), and Cooperative Projects between Undergraduate Universities in Chongqing and Institutes affiliated with Chinese Academy of Sciences (no. HZZ2021014).

References

- [1] X. Wang, "Translation correction of English phrases based on optimized GLR algorithm," *Journal of Intelligent Systems*, vol. 30, no. 1, pp. 868–880, 2021.
- [2] L. Lin, J. Liu, X. Zhang, and X. Liang, "Automatic translation of spoken English based on improved machine learning algorithm," *Journal of Intelligent & Fuzzy Systems*, vol. 40, no. 2, pp. 2385–2395, 2021.
- [3] M. Sofiev and J. Vira, "Construction of an Eulerian atmospheric dispersion model based on the advection algorithm of M. Galperin: dynamic cores," *Geoscientific Model Development Discussions*, vol. 5, no. 3, pp. 1567–1578, 2015.
- [4] M. Mortezaee, M. Ghoatmand, and A. Nazemi, "An application of generalized fuzzy hyperbolic model for solving fractional optimal control problems with caputo–fabrizio derivative," *Neural Processing Letters*, vol. 52, no. 3, pp. 41–44, 2020.
- [5] Z. Chen, Y. Zhao, Z. Wang, Z. Kou, and H. Li, "A novel method for the construction of evolutionary tree based on expectation maximization algorithm," *Journal of Computational and Theoretical Nanoscience*, vol. 13, no. 6, pp. 3799–3803, 2016.
- [6] B. P. Numbi and X. Xia, "Optimal energy control of a crushing process based on vertical shaft impactor – ScienceDirect," *Applied Energy*, vol. 162, pp. 1653–1661, 2016.
- [7] H. M. Hasani, "Gravitational search algorithm-based optimal control of archimedes wave swing-based wave energy conversion system supplying a DC microgrid under uncertain dynamics," *IET Renewable Power Generation*, vol. 11, no. 6, pp. 763–770, 2017.

- [8] C. Chen, J. Li, J. Luo, S. Xie, and H. Li, "Seeker optimization algorithm for optimal control of manipulator," *Industrial Robot: International Journal*, vol. 43, no. 6, pp. 677–686, 2016.
- [9] Y. Sun, "Unsupervised wireless network model-assisted abnormal warning information in government management," *Journal of Sensors*, vol. 2021, Article ID 1614055, 12 pages, 2021.
- [10] F. Guan and Q. Zhang, "A desirability function-based relatively optimal interval core model and an algorithm for fuzzy profit allocation problems of enterprise strategy alliance," *International Journal of Computational Intelligence Systems*, vol. 8, no. 1, pp. 41–53, 2015.
- [11] Apogeeweb, "What is A low pass filter circuit?," 2019, <https://www.apogeeweb.net/article/659.html>.
- [12] Y. Duan, "Construction of first-class university course based on artificial intelligence and neural network algorithm," *Journal of Intelligent and Fuzzy Systems*, vol. 40, no. 12, pp. 1–12, 2020.
- [13] G. Liu, "Construction of ideological education evaluation system for college students -- based on BP neural network model algorithm," *Journal of Physics: Conference Series*, vol. 1852, no. 4, pp. 42074–42084, 2021.
- [14] S. N. Chukanov and E. L. Pershina, "Formation of optimal control of nonlinear dynamic object based on Takagi-Sugeno model," *Computer Research and Modeling*, vol. 7, no. 1, pp. 51–59, 2015.
- [15] D. Jahed Armaghani, E. Tonnizam Mohamad, E. Momeni, M. S. Narayanasamy, and M. F. Mohd Amin, "An adaptive neuro-fuzzy inference system for predicting unconfined compressive strength and Young's modulus: a study on Main Range granite," *Bulletin of Engineering Geology & the Environment*, vol. 74, no. 4, pp. 1301–1319, 2015.
- [16] W. Hong and G. Tonghui, "Training algorithm of adaptive neural fuzzy inference system based on improved SRUKF," *IAENG International Journal of Computer Science*, vol. 44, no. 4, pp. 396–403, 2017.
- [17] D. Li, "Design of English text-to-speech conversion algorithm based on machine learning," *Journal of Intelligent and Fuzzy Systems*, vol. 40, no. 2, pp. 2433–2444, 2021.
- [18] J. Gu and R. Shi, "English teaching quality evaluation based on fuzzy comprehensive evaluation of neural network algorithm," *Dynamic Systems and Applications*, vol. 29, no. 5, pp. 543–563, 2020.